



ISSN: 0976-3376

Available Online at <http://www.journalajst.com>

ASIAN JOURNAL OF
SCIENCE AND TECHNOLOGY

Asian Journal of Science and Technology
Vol. 08, Issue, 01, pp.4078-4083, January, 2017

RESEARCH ARTICLE

EVALUATION OF THERMAL PROPERTIES AND LIFE TIME OF MULTILAYERED THERMAL BARRIER COATING OBTAINED FROM SUSPENSION PLASMA SPRAY

¹Mujeebulla Khan Guttal and ²Abdul Sharief

¹Mechanical Engg, STJIT Ranebennur

²Mechanical Engineering, PA college of Engg Mangalore

ARTICLE INFO

Article History:

Received 20th October, 2016
Received in revised form
27th November, 2016
Accepted 22nd December, 2016
Published online 31st January, 2017

Key words:

Suspension Plasma Spraying,
Thermal Barrier Coating,
Thermal Conductivity,
Thermo-Cyclic Fatigue.

ABSTRACT

The aim of the study was to find the effect of thermal cyclic furnace (TCF) on thermal properties and life time of multilayered TBC obtained from new coating technology called suspension plasma spray (SPS). Porosity and Microstructure of multilayered TBCs before and after thermal aging were analyzed to understand the effect of sintering. Study uses single layer 7% YSZ and Lanthanum Zirconate (LZ) $\text{La}_2\text{Zr}_2\text{O}_7$, double-layer LZ/YSZ TBC deposited with SPS. The overall coating thickness in all TBCs was kept the same. TBC systems were heat-treated in a normal electrically heated furnace at 1100 °C for 150 TCF cycles. Microstructure analyzed using scanning electron microscopy (SEM). Porosity measured using mercury intrusion method at 0, 50,100,150 TCF cycles. Thermal diffusivity, specific heat and thermal conductivity of both single and double layered TBCs analyzed using laser flash analyzer. Porosity has reduced due to sintering with increase in thermal conductivity in both single and double layered TBC. Life time of single and double layered TBC coated SPS has shown better life time. Tests revealed that the double layered SPS LZ/YSZ had improved thermal properties with better life time.

Copyright©2017, Mujeebulla Khan Guttal and Abdul Sharief. This is an open access article distributed under the Creative Commons Attribution License, which permits unrestricted use, distribution, and reproduction in any medium, provided the original work is properly cited.

INTRODUCTION

Thermal barrier coatings (TBCs) used in gas turbine, engines parts for several decade to give thermal insulation to under laying metal parts. A growing demand to improve the fuel economy and higher efficiency with lower harmful emission has led the use of high operating temperature materials (Friedrich *et al* and Tabbara *et al*). Conventional TBCs is a three-layered material system, a substrate material protected from high temperature exposure, an oxidation-resistant metallic bond coat to improve adhesion between metallic substrate and ceramic top coat, and a ceramic top coating deposited on bond coat either by air plasma spray (APS) or suspension plasma spray (SPS) process (Zhu and Fauchais). It is generally noted that the TBC life mainly depends on the properties of bond coat, thermally grown oxide (TGO) which forms during high temperature exposure at the TBC/BC interface (I. Golosnoy, Y. G. Shan and H. Aleksanoglu). TGO formed due to oxidation of bond coat caused by oxygen penetrated through ceramic top coat. The growth rate of the TGO and its layer adherence to the metallic bond coat (BC) considered as crucial properties governing the thermal fatigue life of the TBC's during thermal cycling (F. Guo *et al*). Growth of TGO minimize by resisting penetration of oxygen and forming a low thermal conductive coat.

Yttria stabilized zirconia (YSZ) is standard top coat due to its combination of properties and robust record of performance. But it undergoes significant sintering at higher temperature leading to early coating spallation not desired (A. M. Limarga and S. R. Choi). Lanthanum zirconate $\text{La}_2\text{Zr}_2\text{O}_7$ (LZ) is alternate to overcome this drawback and become interesting due to its low thermal conductivity. However, due to low fracture toughness of YSZ and high tendency of LZ to react and degrade with aluminium a single layered TBC is not much beneficent. To have better life time and to over the drawbacks of single layer, a multilayered TBC with LZ on top of YSZ is used in present study. Atmospheric plasma spray (APS) is most commonly used method for coating. Ease of coating and unique micro structural characteristics has made APS as most commonly used method (C. G. Levi, Curry, N). APS process uses a plasma jet to melt the feedstock powder into droplets sprayed onto the substrate. Since the process produces non columnar structure and sintering effect at high temperature exposure reduces life time of TBC. The newly developed suspension plasma spray (SPS) has emerged as a potential candidate for depositing TBCs as it produce columnar microstructure with high deposition rate and combines the benefits of both APS and EB-PVD. SPS uses liquid feedstock with ethanol as carrier in which the powder suspended. Liquid feedstock atomized and admitted in plasma flame and targeted on the substrate (D. Naumenko *et al.*).

*Corresponding author: Mujeebulla Khan Guttal,
Mechanical Engg, STJIT Ranebennur.

Experimental Procedure

Preparation of Substrate and bond coat

The investigated TBC systems were deposited on nickel based high temperature alloys like super alloy IN738. Circular shape discs of diameter 25mm with thickness of 5mm(25mm x5mm) were grit blasted using abrasive alumina particles of 200 sizes to create a required surface roughness Rapro file of 5 μm . Atmospheric plasma spraying was used to deposit NiCoCrAlY composition (AMDRY 9951) m using the Sulzer Metco F4gun. A standard $200 \pm 20 \mu\text{m}$ bond coat on grit blasted surface was maintained same for all samples. Bond coat surface roughness was measured using profile projector as $7\mu\text{m}$ on Ra Scale.

Preparation of top coat

The ceramic top coat is the component which gives a TBC system its thermal insulation to the substrate (D. Naumenko). Samples were prepared using coating method suspension plasma spraying (SPS) with different coating layers as single layer, double layer and triple layer (P. Fauchais). Suspension plasma spraying (SPS): For the present work, two different stabilizers with two suspensions were prepared to produce multilayer TBC. Ethanol was used as carrier in which the lanthanum zirconate of mean particle size 400nm with 30wt % of solid load is suspended. Other suspension was 7% partially stabilized zirconia (7YPSZ) with mean particle size of 400nm dispersed in alcohol with solid load of 30wt%. Suspension were sprayed using MF-4MB spray gun along with an atomizer with Nan feed suspension feeding system. A standoff distance of 100mm with total gas flow of 250-300lt/min was maintained to produce single layer and double layer specimens. Denser triple layers with columnar structure on specimen were produced by keeping higher enthalpy and lower gas flow rate of SPS

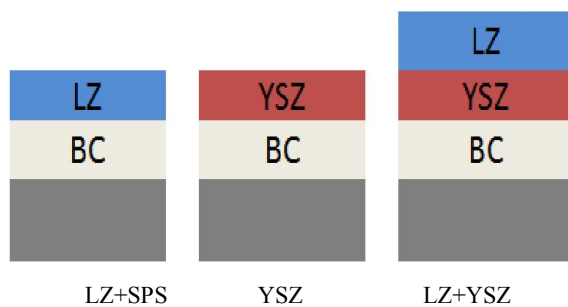


Fig.1. TBCs produced for the present study

Three variations in the top ceramic coating structure were produced as shown in Fig.1. The variation was a layer coating of lanthanum zirconate (LZ) with a thickness of 200 μm produced by SPS. Third variation was a double-layered ceramic coating comprising of LZ (250 μm thick) as the top coat on YSZ base layer (100 μm thick) produced by SPS. Bond coats were coated with High Velocity Air Fuel (HVAF) with Three variations were prepared using Suspension plasma spray (SPS) one with columnar ceramic top coat of YSZ (200 μm) and other was columnar ceramic coat of LZ (250 μm). Third SPS variation comprises of top coat LZ (250 μm thick) on YSZ base layer (100 μm).

Coating Characterization

All the selected specimens before and after cyclic thermal exposure were preprocessed to observe the microstructure and mechanical properties. The specimens were sectioned using slow speed diamond cutting blade. Polishing was done using 220 grit, 140 grit size discs successively and then with diamond paste of 9 micron, 6 micron, 3 micron respectively. Final polishing step was carried out on 0.05 micron silica paste until a scratch free mirror finished surface was obtained. The microstructures of the TBC specimens were observed using a scanning electron microscope (SEM; Model JSM-5610, JEOL, Japan)

Porosity Measurements: The sample chosen for the porosity assessment were prepared by cutting and grinding with abrasive paper (gradation 200, 400, 600), followed by polishing on diamond pastes according to the standard procedure (G.J. Yang at all and Hille *et al*). Before the test the coating was removed and washed with water and heated in furnace about 1200 C for 30min to remove the absorbed water (K. von Niessen *et al*). A force was exerted to make mercury to intrude in pores. The volume of mercury that enters pores is measured by a mercury penetrometer (an electrical capacitance dilatometer). These devices are very sensitive and can detect a change in mercury volume of under 0.1 μL (Gong, K at al).

Density measurement: The SPS coated specimens coating density (ρ) was obtained by direct measurement of the weight of the substrate with and without the coating. The experimental error was affected by roughness of bond coat and the measurement of the coating thickness and the weight were taken about $\pm 2.5\%$ (P.-C. Tsai at al). SPS coated specimens were sectioned and are projected in 300X magnification SEM micrographs. A horizontal straight line is drawn passing through the coating thickness. The gaps and intercepting line were considered. Same micrographs of 25 were considered for the column density measurements and the average values for each difference are reported.

Measurement of thermal properties

Thermal diffusivity: Disc of 10mm diameters were cut from coated plate by water jet. To measure thermal diffusivity laser flash analysis (LFZ) NETZSCH 467 was used. The samples were coated with thin layer of graphite to improve absorption of laser light. Rear surface of the 10mm diameter sample was exposed to a laser of known pulse width and front face was placed with Insbinfra-red detector to record the rise in temperature.

$$\alpha = (0.1388 * d^2) / t_{0.5} \quad (1)$$

The response is normalized and thermal diffusivity (α) calculated from the above formula. Where α is thermal diffusivity (mm²/sec), d is the thickness of sample and $t_{0.5}$ is the half time taken for rise in temperature measured by LFA.

Specific heat capacity: A Differential Scanning Calorimeter 404C was used to establish the specific heat capacity of the coatings. Sapphire was used as the reference to evaluate the specific heat capacity.

Thermal conductivity: with the value of specific heat C_p and thermal diffusivity using following equation the thermal conductivity was found. The accuracy of thermal conductivity depends on the variables of equation.

$$k = \alpha(T) * c_p(T) * \rho(T) \quad (2)$$

Thermal Aging: Thermal aging is process of heating TBC coated specimens at high temperature mimic the actual working environment.

There a mainly three types of thermal aging namely 1) Thermal cyclic furnace (TCF) 2) Isothermal thermal aging 3) Burner test rig (BTR). Present work carried out using thermal cyclic furnace includes heating for one hour at 1100C and cooling outside by forced air for 10min to reach temperature to reach 1000C. For study purpose 150cycles of TFC tested to measure thermal properties. Further thermal aging continued to notice first spallation of top coat to note as life time.

RESULTS AND DISCUSSION

Microstructure: The microstructure of all polished thickness of coatings produced by SPS before aging are investigated using SEM and the microstructure features of the analyzed coatings are shown in following fig. 2, 3, 4

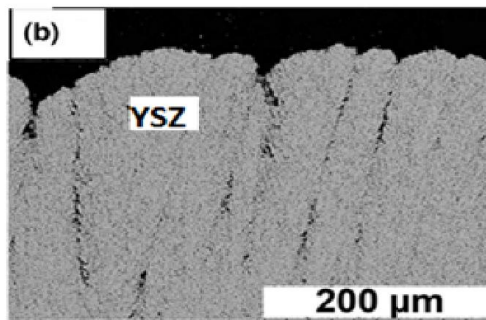


Fig. 2. SEM images of cross section of Single layer YSZ prepared by SPS

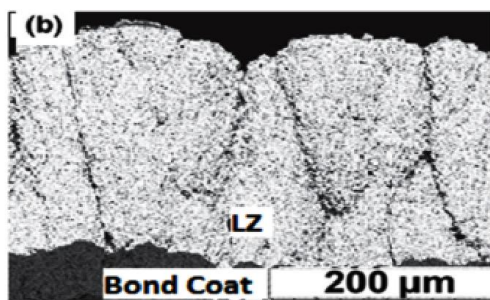


Fig. 3. SEM images of cross section of Single layer LZ prepared by SPS

Uniformly distributed columnar structure with porosity and column gaps was observed in the cross-sectional microstructure of Single layer prepared by SPS was observed in fig. 2 Fig. 3 shows the SEM micrographs of single layer TBC with top coat as LZ. Micrograph reveals the same pattern of micrographs as observed in previous case of Single layer YSZ prepared by SPS. A Cross sectional SEM micrographs of Double layer top coat comprising 100 μ m of YSZ over which a 200 μ m of LZ is as shown in fig.4

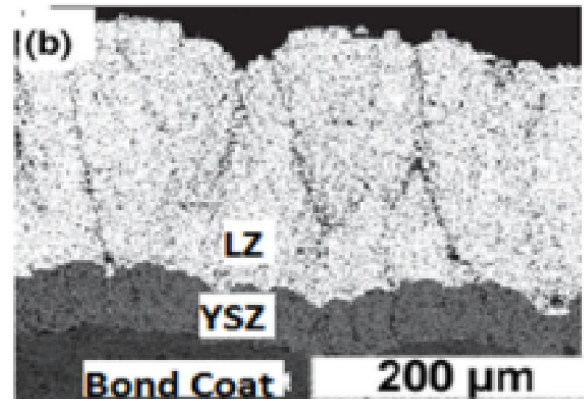


Fig. 4. SEM images of cross section of Double layer prepared by SPS

The average total thickness of ceramic coating was approximately $300 \pm 20 \mu\text{m}$ which included both YSZ and LZ. SPS samples with double layer show a columnar structure of LZ originated from YSZ layer. The columns are regular with pores distributed evenly as shown in cross sectional micrographs.

Effect of thermal aging on microstructure: The cross-sectional SEM micrographs after 150cycles of thermal cyclic fatigue are shown in figure. The Thermally grown oxides (TGO) in SPS system was formed at the ceramic/bond-coat interface due to oxygen penetration through the top ceramic layer. When the oxidation properties of the single layered coating with different coating methods are compared, it was cleared that the porosity of SPS are at column gaps and are widely distributed. Regular column gaps of SPS leads to greater porosity form low thermal conductivity to form thin TGO as shown in Fig 5

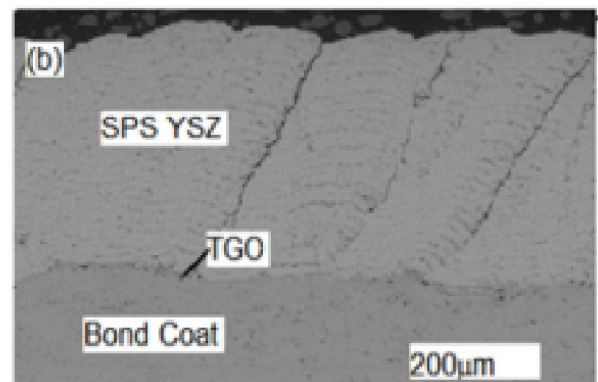


Fig. 5. Cross sectional SEM images of single layered YSZ TBC after thermal aging for 150cycles produced a) APS b) SPS

The cross sectional SEM micrographs of Single layered TBC with TC as LZ coated with SPS after thermal aging are shown in Fig 6(a) (b).Microstructures of single layered LZ coated specimens show similar as YSZ in SPS coated samples. TGO was found much thicker in case of single layered YSZ than in LZ single layered. Double layer TBC having YSZ on bond coat over which a layer of LZ was coated using APS and SPS coating methods. Cross sectional SEM images of double layer coated specimens are shown in fig. 7it is clear that the specimens have lower oxidation causing thin TGO at interface of bond coat in bi-layer SPS coated specimens.

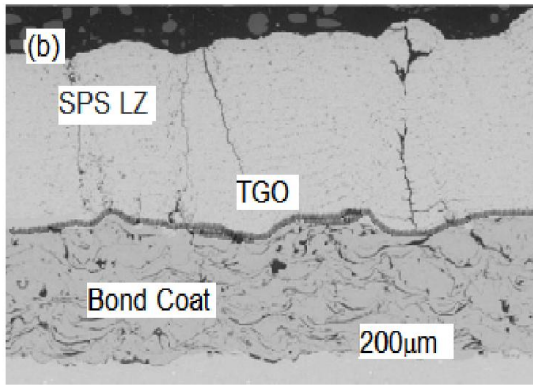


Fig.6. Cross sectional SEM images of single layered LZ TBC after thermal aging for 150cycles produced SPS

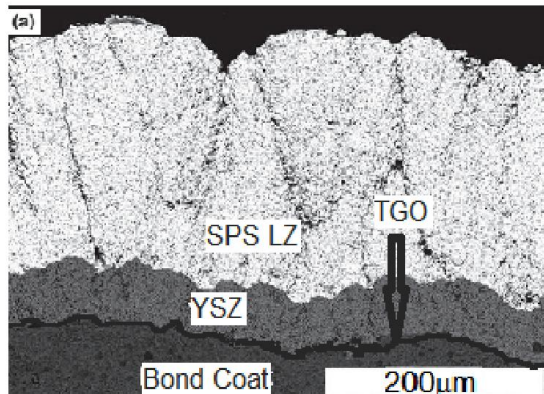


Fig.7. Cross sectional SEM images of Double layered YSZ and LZ TBC after thermal aging for 150cycles produced SPS

Thermal diffusivity: Thermal diffusivity of different specimens obtained from the laser flash analysis equipment is plotted in Fig. 8. The thermal diffusivity of single and double layered ceramic system was calculated by considering the entire ceramic system as a single unit. Measurements were made for all TBCs at different temperature as shown in fig.8 Error in diffusivity measurements were considered to be ±2% as claimed by the equipment suppliers.

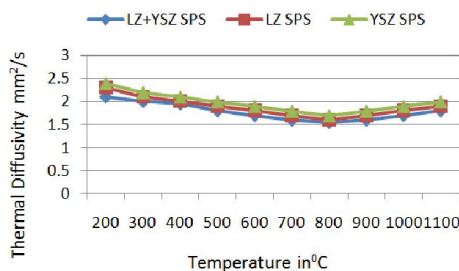


Fig. 8. Thermal diffusivity v/s temperature

The trend of diffusivity change is as shown Fig where for SPS specimens have increase in thermal diffusivity with increase in temperature for all three coatings. Specimen with double layer TBC having top coat LZ+YSZ coated with APS shows low thermal diffusivity. LZ and YSZ layer at top forms porous media causing drop on thermal diffusivity. Thermal diffusivity in case of all TBCs coated with SPS show decreases initially and increases at about 8000C to 10000C.

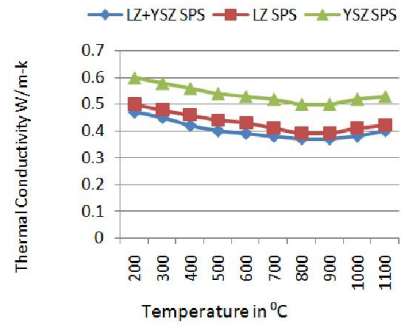


Fig. 9. Thermal conductivity versus temperature plot of the TBCs

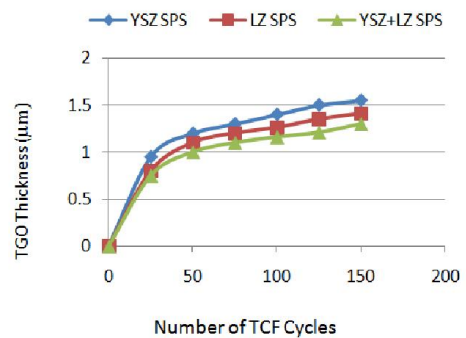


Fig. 10. Thickness of TGO verses number TCF cycles

This may be due to sintering of ceramic structure begins to occur above 8000C causing an increase in thermal conductivity. TBC with top coat LZ and YSZ shows less thermal diffusivity among all other coatings.

Thermal conductivity: Experimental values of thermal diffusivity, specific heat capacity and density are utilized to obtain thermal conductivity by using an equation (2). Fig 9 shows thermal conductivities of 3 different coatings prepared by two coating methods. Thermal conductivities of coating show initial decrease with temperature and a steep jump in conductivities can be seen after 10000C. It can be seen that the trend among all the coatings at all temperatures is similar, which is increase in thermal conductivity with increase in temperature beyond 9000C. The reason for increase in conductivity can be because of less porosity after 9000C generated by SPS coating method.

The trend can be because of columnar gaps and pores constituting fall in conductivity. Double layered sample with LZ+YSZ top coat, coated with SPS coating was found to be the lowest thermal conductive sample.

Thickness of TGO: The thickness of the TGO layer at bond coat and top coat interface was measured after oxidation for 150TCF cycles at 1100°C. Thickness of TGO was measured to determine TGO growth at interface. TGO thickness was measured using SEM micrographs at more than 20 locations and average value was taken as TGO thickness. Fig 10 shows TGO growth against the number of oxidation cycles for 6TBC coatings. TGO thickness was observed more growth in single layered YSZ coated specimen in comparison with other TBCs.

It may be seen that the growth of TGO layer approximately followed a parabolic relationship. Approximately till 30 cycles the growth was rapid and becomes gradually constant after 100 cycles. SPS single layer sample have thick TGO because of columnar gaps and pores allowing more oxygen to bond coat for oxidation. Dual layer LZ+YSZ coated with SPS show low TGO thickness among other SPS coated samples.

Porosity measurement: Porosity was measured using mercury intrusion method. Mercury was forced to intrude in the pores and gaps present in coating and the volume of mercury was considered to determine porosity. Porosity of APS coated and SPS coated specimens before oxidation and after oxidation are plotted in figure.11 double layered coated samples show less porosity than Single layered samples. In SPS samples columnar structure contribute columnar gaps and pores creating high porosity. Porosity has reduced with increase in oxidation from as sprayed to 150TCF cycles. A possible explanation for this reduced porosity could be because of sintering with exposure to heat treatment.

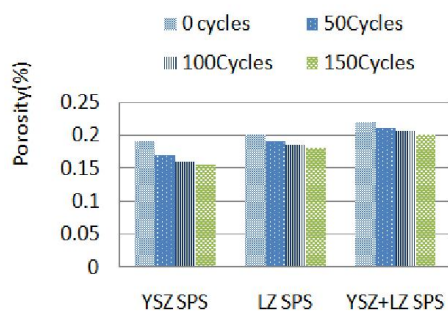


Fig. 11. Porosity formed with number of TCF Cycles

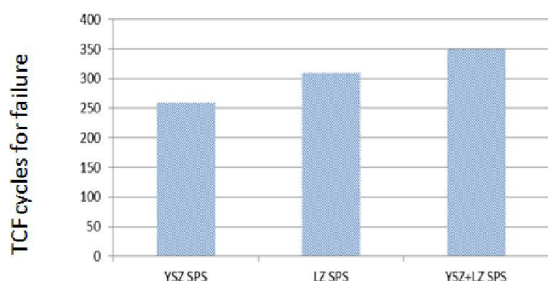


Fig. 12. Life time different TBC coatings

Thermal fatigue life: Fig 12 Shows thermal fatigue life of all TBC samples tested at 1100°C until the top coat of TBC spalled. It was observed that YSZ single layered TBC show least life time about 250TCF cycles whereas other TBC show better life time. A possible reason for low TBC life in case of single coated specimens could be high conductivity of heat causing thermal mismatch leading to crack nucleation. LZ APS show 70cycles improved in life time and double layer TBC forms better insulation to oxygen penetration and reduced thermal conductivity causing long life time of about 300cycles. In double layered SPS coated samples show improved life time. Single layered YSZ show similar life time as that of LZ slightly improved life time, whereas in double layer LZ+YSZ showed improved life time than single layered. A reason for this improved life time can be densely packed columnar structure creating low thermal conductivity and resistance to oxygen penetration to reach bond coat for oxidation.

Double layered LZ+YSZ SPS specimens show better life time among all other specimens where a top layer of LZ act as resistance to oxygen penetration and second layer of columnar YSZ having pores and gaps forms low thermal conductive layer. Failure in double layer LZ+YSZ SPS occurred at interface with YSZ and bond coat. Reason for such failure may be due to the CTE mismatch by YSZ and bond coat.

Conclusions

Three different TBCs (YSZ, LZ and LZ+YSZ) prepared with two coating methods (APS and SPS). Tested for their functional performance under thermal cyclic furnace at 1100°C and conclusions were drawn as follows SPS coating method produces columnar structure with high porosity leading to low thermal conductive of top coat whereas APS coating produces splats structure with low porosity.

- LZ show better life time than YSZ with SPS
- coating, dual layer with LZ+YSZ was found to perform well among other coatings with SPS coating method. A possible reason for this can be due to reduced thermal conductivity with resistance to penetration of oxygen.
- Microstructure analysis reveals that crack nucleation in all TBCs is at interface between bond and ceramic top coat which because of mismatch in CTE and oxidation of bond coat leading to TGO growth.
- A dual layered TBC with LZ+YSZ coated with SPS gives long thermal fatigue life and a dual layer TBC is beneficent than single layer TBC.

Acknowledgements

The authors are grateful to NITK surathkal for providing test facilities and also would like to thank MEP Bangalore for providing coating facilities.

Conflict of interest

The authors declare no conflict of interest.

Funding

This research received no specific grant from any funding agency in the public, commercial or not-for-profit sectors.

REFERENCES

- A New Material for Atmospheric Plasma Spraying of Advanced Thermal Barrier Coatings, (C. Friedrich, R. Gadow, and T. Schirmer, Lanthanum HexaaluminateJ. Therm. Spray Technol., 2001, 10(4), p 592-598)
- A study of liquid droplet disintegration for the development of nanostructured coatings (H. Tabbara and S. Gu, AICHE J., vol. 58, no. 11, pp.3533–3544, Nov. 2012)
- A study of the microstructure and oxidation behavior of alumina/yttria-stabilized zirconia (Al₂O₃/YSZ) thermal barrier coatings (C. Zhu, A. Javed, P. Li, F. Yang, G. Y. Liang, and P. Xiao Surface and Coatings Technology, vol.212, pp. 214–222, Nov. 2012)
- A. Key challenges and opportunities in suspension and solution plasma spraying (Fauchais, P.; Vardelle, M.;

- Goutier, S.; Vardelle Plasma Chem. Plasma Process. 2015, 35, 511–525)
- An analytical model for simulation of heat flow in plasma-sprayed thermal barrier coatings,” *Journal of Thermal Spray Technology* (I. Golosnoy, S. Tsipas, and T. Clyne vol. 14, no. 2, pp. 205–214, Jun. 2005)
- Analysis of deposits formation in plasma spraying with liquid precursors (Y. G. Shan, Y. L. Wang, and T. Coyle *Appl. Therm. Eng.*, vol. 51, no. 1–2, pp. 690–697, Mar. 2013)
- Determining a critical strain for APS thermal barrier coatings under service relevant loading conditions,” *International Journal of Fatigue* (H. Aleksanoglu, A. Scholz, M. Oechsner, C. Berger, M. Rudolphi, M. Schütze, and W. Stamm vol. 53, pp. 40–48, Aug. 2013)
- Effect of Fe₂O₃ doping on sintering of yttria-stabilized zirconia (F. Guo and P. Xiao *Journal of the European Ceramic Society*, vol. 32, no. 16, pp. 4157–4164, Dec. 2012)
- Effect of hightemperature aging on the thermal conductivity of nanocrystalline tetragonal yttria-stabilized zirconia (A. M. Limarga, S. Shian, M. Baram, and D. R. Clarke) *Acta Materialia*, vol. 60, no. 15, pp. 5417–5424, Sep. 2012)
- Effect of Sintering on Mechanical Properties of Plasma-Sprayed Zirconia-Based Thermal Barrier Coatings (S. R. Choi, D. M. Zhu, and R. A. Miller) *J. Am. Ceram. Soc.*, 88 (10) 2859–67 (2005).
- Environmental Degradation of Thermal-Barrier Coatings by Molten Deposits (C. G. Levi, J. W. Hutchinson, M. H. Vidal-Setif, and C. A. Johnson *MRS Bull.*, 37 (10) 932–41 (2012)
- Evaluation of the lifetime and thermal conductivity of dysprosia-stabilized thermal barrier coating systems (Curry, N.; Markocsan, N.; Östergren, L.; Li, X.-H.; Dorfman, M.J. *Therm. Spray Technol.* 2013, 22, 864–872)
- Evaluation of the Lifetime and Thermal Conductivity of Dysprosia-Stabilized Thermal Barrier Coating Systems (N. Curry, N. Markocsan, L. Ostergren, X.H. Li, and M. Dorfman *J. Therm. Spray Technol.*, 2013, 22(6), p 864–872)
- Failure Mechanisms of Thermal Barrier Coatings on MCrAlY-Type Bondcoats Associated with the Formation of the Thermally Grown Oxide (D. Naumenko, V. Shemet, L. Singheiser, and W. Quadackers *J. Mater. Sci.*, (7) 1687–703 (2009))
- Influence of bond coat surface roughness on the structure of axial suspension plasma spray thermal barrier coatings—Thermal and lifetime performance (Curry, N.; Tang, Z.; Markocsan, N.; Nylén, P. *Surf. Coat. Technol.* 2015, 268, 15–23)
- Latest Developments in Suspension and Liquid Precursor Thermal Spraying (P. Fauchais and G. Montavon *J. Therm. Spray Technol.*, vol. 19, no. 1–2, pp. 226–239, Jan. 2010)
- Microstructural and Mechanical Property Evolutions of Plasma-Sprayed YSZ Coating during High-Temperature Exposure: Comparison Study between 8YSZ and 20YSZ (G.J. Yang, Z.L. Chen, C.X. Li, and C.-J. Li *J. Therm. Spray Technol.*, 2013, 22(8), p 1294–1302)
- Oxidation-induced stresses in thermal barrier coating systems. In *Advanced Ceramic Coatings and Interfaces V: Ceramic Engineering and Science Proceedings*; (Zhu, D., Lin, H.-T., Mathur, S., Ohji, T., Eds.; John Wiley & Sons, Inc.: Hoboken, NJ, USA, 2010; Volume 31, doi:10.1002/9780470943960.ch3)
- Oxide growth and damage evolution in thermal barrier coatings. (Hille, T.S.; Turteltaub, S.; Suiker, A.S. *J. Eng. Fract. Mech.* 2011, 78, 2139–2152)
- Plasma Spray-PVD: A New Thermal Spray Process to Deposit Out of the Vapor Phase (K. von Niessen and M. Gindrat *J. Therm. Spray Technol.*, vol. 20, no. 4, pp. 736–743, Apr. 2011.)
- Process diagnostics in suspension plasma spraying (G. Mauer, A. Guignard, R. Vaßen, and D. Stöver *Surface and Coatings Technology*, vol. 205, no. 4, pp. 961–966, Nov. 2010)
- Thermal conductivity and lifetime testing of suspension plasma-sprayed thermal barrier coatings (Curry, N.; VanEvery, K.; Snyder, T.; Markocsan, N. *Coatings* 2014, 4, 630–650.)
- Thermal cyclic oxidation performance of plasma sprayed zirconia thermal barrier coatings with modified high velocity oxygen fuel sprayed bondcoatings (P.-C. Tsai, C.-F. Tseng, C.-W. Yang, I.-C. Kuo, Y.-L. Chou, and J.-W. Lee *Surface and Coatings Technology*, vol. 228, Supplement 1, pp. S11–S14, Aug. 2013)
- Trice, Microstructure and thermal properties of inflight rare-earth doped thermal barriers prepared by suspension plasma spray (Gong, K.; VanEvery, H.; Wang, R.W. *J. Eur. Ceram. Soc.* 2014, 34, 1243–53)
